Article

Adsorptive Removal of As(III) by Cellulose-Sn(IV) Biocomposite

Anita Shekhawat [1], Ravin Jugade [1,*] , Vaishnavi Gomase [1], Shashikant Kahu [1], Saravanan Dhandayutham [2] and Sadanand Pandey [3,*]

[1] Department of Chemistry, Rashtrasant Tukadoji Maharaj Nagpur University, Nagpur 440033, Maharashtra, India
[2] Department of Chemistry, National College (Autonomous), Tiruchirapalli 620001, Tamilnadu, India
[3] Department of Chemistry, Yeungnam University, Gyeongsan 38541, Gyeongsangbuk-do, Republic of Korea
* Correspondence: ravinj2001@yahoo.co.in (R.J.); sadanand.au@gmail.com or spandey@ynu.ac.kr (S.P.)

Abstract: Cellulose-Sn(IV) (CSn) biocomposite was synthesized by cellulose and stannic chloride in ethanol medium using microwave irradiation for 2 min with 30 s of intermittent time intervals. The incorporation of Sn(IV) into the cellulose matrix was confirmed through FT-IR, XRD, TGA, SEM- EDS, and BET. The prepared composite CSn has been used for the adsorptive removal of As(III) from water. Parameters, such as initial concentration, adsorbent dose, initial As(III) concentration, and time required for the adsorption process, were optimized through the batch-adsorption process. The adsorption capacity of the CSn for As(III) adsorption was found to be 16.64 mg/g at pH 7.0. Freundlich isotherm was found to be more suitable for the adsorption process based on regression coefficient values. Pseudo-second-order kinetic model was found to be more suitable for understanding the kinetics of the adsorption of As(III). Weber–Morris model with non-zero intercept revealed that the mechanism of adsorption was not limited to the diffusion process only. The adsorption process was spontaneous and exothermic and showed a decrease in randomness. Chloride ions decreased the percentage removal of As(III) when the concentration of chloride ions was ten times that of As(III) concentration according to the results obtained through the effect of co-anions study. In this study, 5% (w/v) NaCl solution has been used for the regeneration of the material, and during up to five adsorption–desorption cycles, there was a gradual decrease in percentage removal of As(III) from 95% to 78% only, which proves the greener aspect of the CSn. The breakthrough volume of 1.25 L of 10 mg/L of As(III) in column studies revealed that the CSn could be applicable for larger sample volumes also.

Keywords: Biocomposite; cellulose; Sn(IV); adsorption; As(III); regeneration

1. Introduction

Cellulose is the most abundant biopolymer available in nature [1]. The presence of hydroxyl functional groups in its structure provides reactive sites for the introduction of various organic and inorganic moieties in its matrix [2]. The structural modification changes the chemical and physical properties of the native cellulose [3]. Modified biopolymeric materials have wide applications in various industries as well as for environmental remediation [4]. In the literature, it was reported that biopolymers could be used as host matrixes for the immobilization of multivalent metal ions and as potent adsorbents [5,6]. Tin exists in (+2) and (+4) oxidation states and has a tendency to react with organic functionalities easily. Tin-based composites have been reported in the literature for the adsorption of dyes and hazardous ions effectively [7]. The combination of tin with biopolymers is a greener opinion to treat toxic waste in a synergistic manner, as tin provides stability and reactive property to the biocomposites, and a dense network of biopolymers avoids the leaching of tin into the water. In other words, this is the way to take advantage of tin properties in an eco-friendly manner [8].

Arsenic (As) is generally found in surface water around geothermal-active areas. In contamination of groundwater, the main sources of arsenic are base metal sulfides, ar-

senopyrite, and realgar. As(III) and As(V) exist in water in the form of oxyanions. However, As(III) is more mobile and toxic than As(V) [9]. Consumption of arsenic-contaminated water leads to arsenicosis and cancer in the skin, lungs, or kidneys. Sometimes, consumption of arsenic-contaminated water gives rise to diabetes, hypertension, and reproductive disorders [10]. The permissible limit of Arsenic in drinking water is 10 µg/L, according to World Health Organization (WHO) guidelines. In India, groundwater of some regions of Bihar, West Bengal, Uttar Pradesh, Jharkhand, Manipur, Assam, and Chhattisgarh states have an arsenic concentration of more than the permissible limit [11]. So, there is a need for an effective methodology for the removal of arsenic from water bodies. The adsorption process has been reported as the most effective method reported for the reduction of arsenic levels in water [12,13].

By considering the above perspective, cellulose- and tin-based biocomposite has been synthesized within a short period of time by using microwave irradiation. The prepared material was used for the adsorption of As(III) from water with optimized conditions.

2. Materials and Methods

All the chemicals used for synthesis and adsorption studies were of analytical grade (AR) and procured from SRL Chemie Ltd., India. A stock solution of As(III) of 1000 mg/L was prepared by dissolving 1.32 g of As_2O_3 in 1.0 M NaOH(25 mL) and diluting it to 100 mL. The solution obtained was neutralized with 1.0 M HCl by using 0.2% phenolphthalein (2 drops), and further volume made up to 1 L. Working standard solutions of various concentrations of As(III) were prepared from the stock solution for adsorption studies.

A homogeneous mixture of 2 mL anhydrous Sn(IV) chloride and 4 g of microcrystalline cellulose dispersed in 30 mL methanol was obtained by stirring. The mixture was exposed to microwave irradiation for 2 min with 30 s of the time interval. The resultant precipitate was centrifuged and washed with distilled water. The washing was continued till the negative test for chloride ions was obtained and then dried in a hot-air oven for 24 h. For the leaching of Sn(IV), 0.5 g of dried material was stirred for an hour with 100 mL distilled water by magnetic stirrer and filtered. The concentration of Sn(IV) ions was detected in the filtrate by ICP-AES, and it was found below the detection limit. The prepared CSn biocomposite has been used for further adsorption studies.

The batch-absorption method was carried out for the adsorption studies [14]. For this, the optimized dose of 400 mg of CSn was stirred with 50 mL of 5–100 mg/L As(III) solutions on magnetic stirrers for 45 min for equilibration. The amount of As(III) was adsorbed (q_e) in mg/g on CSn, and percentage removal capacity was calculated, as given in equation 1 and equation 2, respectively.

$$q_e = \frac{C_0 - C_e}{W} \times V \qquad (1)$$

$$\%Removal = \frac{C_0 - C_e}{C_0} \times V, \qquad (2)$$

where C_0 and C_e indicate the concentrations (mg/L) of As(III) at initial and equilibrium conditions in the solution phase, respectively. V is the volume (L) of As(III) solution in liters. W is the weight(g) of CSn. To obtain reliable results, all the experiments were performed in triplicate. After the adsorption process, ICP-AES analysis for tin was performed to check whether it would leach out in the solution. The result obtained was found to be negative.

FT-IR spectra of native cellulose and CSn were recorded in the wavelength range of 500–4000 cm^{-1} using Bruker Alpha spectrometer with ZnSe ATR crystal. Rigaku Miniflex 300 X-ray diffractometer gives the XRD spectra in 2θ range 3.0–90.00 using copper Kα radiation. Scanning Electron Microscope (SEM) model TESCAN VEGA 3 SBH was utilized for observing the change in the structure of the adsorbent. Elemental composition was confirmed by X-ray analyzer Oxford INCA Energy 250 EDS System. TGA and DTA were recorded by Shimadzu DTG 60 with a scan rate of 20 °C/min in a nitrogen medium. The Brunauer–Emmet–Teller (BET) surface-area measurement was carried out by Quan-

tachrome Nova 2200e. Microwave oven LG, India, with model number MS2049, was used for irradiation during the synthesis of CSn. The concentration of the arsenic in the solution after adsorption was measured using ICP-AES (Thermo IRIS Intrepid II XDL).

3. Results and Discussion

3.1. Characterization of SnC

Figure 1a shows the FTIR spectrum of cellulose having a broad peak of OH stretching at 3370 cm^{-1}. The vibrations of C–O–C bonds were assigned to peak at 1028 cm^{-1}. C–O stretching and bending vibrations were allotted to peaks at 1510 and 1266 cm^{-1}, respectively [15,16]. The peak at 1387 was assigned to C–O–H vibration [17]. Figure 1b shows the spectrum of CSn adsorbent showing characteristic peaks of O–H, C–H, and C–O stretching vibrations at 3370, 1690, and 1028 cm^{-1}, respectively. A new peak at 757 cm^{-1} owing to the stretching vibrations of Sn–O confirmed that the Sn(IV) atoms were present in the network of cellulose chains [8,18]. After the adsorption of arsenic, a new peak was observed at 834 cm^{-1} and a change in the region at 1300–1400 cm^{-1}, which confirms the interaction of Arsenic with the CSn [19].
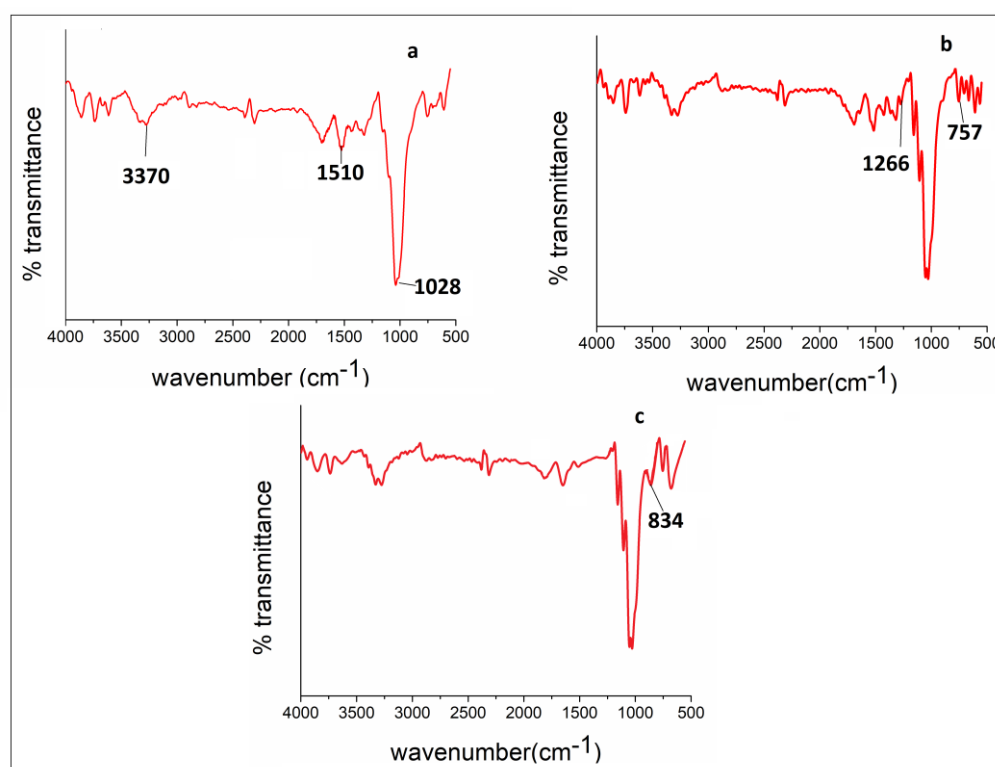
Figure 1. FT-IR of (**a**) Cellulose, (**b**) CSn, and (**c**) CSn with adsorbed As(III).

The observed X-ray diffraction (XRD) patterns of cellulose and CSn are shown in Figure 2. Cellulose biopolymer shows diffraction peaks at 2θ = 14.88° and 22.26° [11]. In CSn, three new peaks at 2θ = 27.1°, 34.5°, and 51.44° have been observed, which matched with the reported peaks of Sn(IV) and confirmed the incorporation of Sn(IV) into the cellulose matrix [20]. Low intensity and broadened peaks are characteristics of amorphous behavior. The decrease in crystallinity of adsorbent can be attributed to the typical amorphous regions of cellulose which are introduced through intramolecular and intermolecular H-bonding interactions and rearrangement [21].
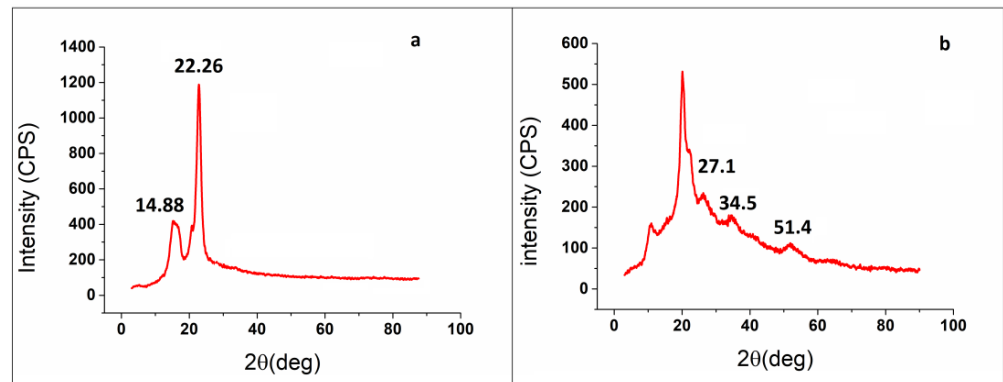
Figure 2. XRD pattern of (**a**) cellulose and (**b**) CSn.

The TGA studies (Figure 3a) of cellulose showed that a weight loss of 3% was observed at 120 °C due to loss of moisture. Further decrease in weight percent was observed with the successive increase in temperature. The overall decomposition of cellulose was observed in two stages. The first degradation curve was observed between 250–390 °C with 85% weight loss from the initial weight of cellulose. The second curve was obtained in the range of 390–650 °C with 95% of weight loss from the initial weight [22]. The same two-stage process was reflected in two exothermic peaks of DTA thermograms presented in Figure 3b. In the case of CSn, it starts degrading below 200 °C because of its amorphous behavior [23]. Such type of degradation behavior was reported in the literature for the cellulose iron-oxide nanocomposites [24]. It was clearly observed that the biocomposite is thermally stable with a total weight loss of 75% at 800 °C compared to cellulose which attributes to the existence of tin (IV) in the biopolymer matrix [25].
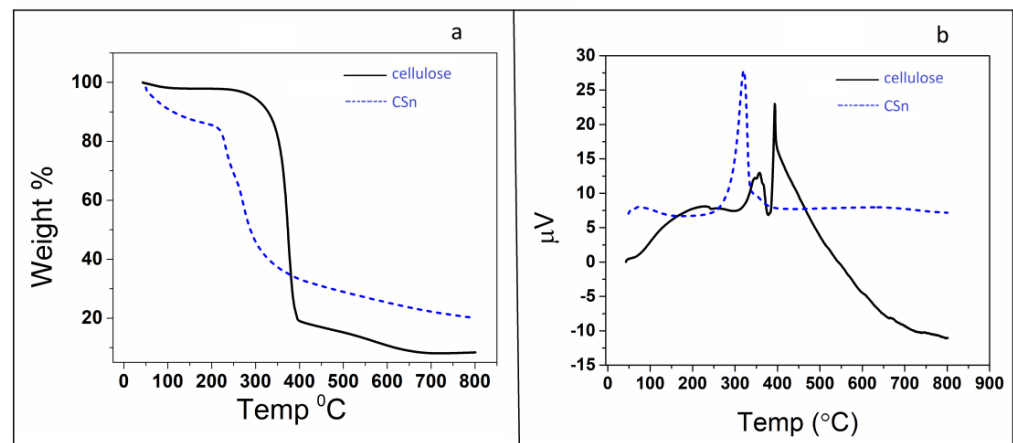

Figure 3. (**a**) TGA curve and (**b**) DTA Curve.

SEM and EDS (Figure 4) of cellulose, CSn, and CSn with adsorbed As(III) were observed to predict the change in structural specifics. The cellulose shows an intense network of fibrous morphology. In CSn, the surface becomes denser with patches. The change in the surface morphology confirms the formation of the biocomposite. The elemental peaks of Sn with peaks of C and O in the EDS Spectrum of CSn confirmed the incorporation of Sn(IV) in the cellulose structure. The adsorption of As(III) on CSn was clearly observed in the EDX spectrum, which showed the arsenic peak with other elemental peaks of CSn.
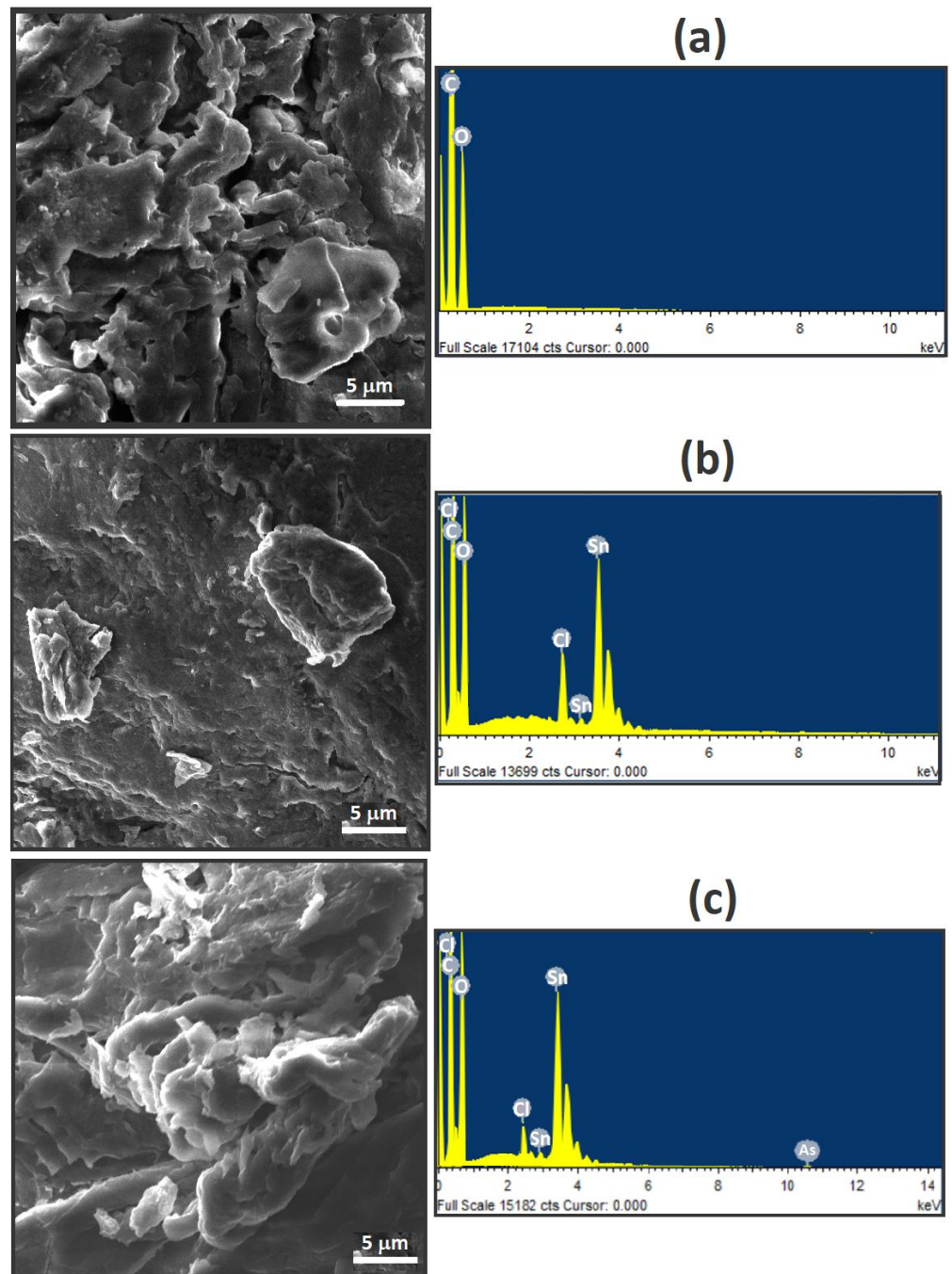
Figure 4. SEM micrograph EDX spectra of (**a**) cellulose, (**b**) CSn, and (**c**) CSn after adsorption of As(III).

The BET surface area of cellulose and CSn were obtained by adsorption–desorption of nitrogen at 77 K. The increase in the surface area from 0.092 to 3.205 m^2/g was ascribed to the collaboration of Sn and cellulose in biocomposite.

3.2. Parameter Optimization

3.2.1. Effect of Time

Contact time was varied from 5–60 min to study the effect of contact time simultaneously on the % removal of As(III) and on the adsorption capacity of CSn. For that purpose, 50 mL of 5 mg/L of As(III) initial concentration equilibrated with 200 mg CSn at 298 K. It was observed that with the increase in time, there was a sudden increase in % removal of As(III) and the adsorption capacity of CSn. At the initial time of 5 min, there were

more available adsorption sites on the CSn surface, and in 45 min, it reached equilibrium (Figure 5a) since, at this stage, most of the adsorption sites were loaded with As(III) [26].
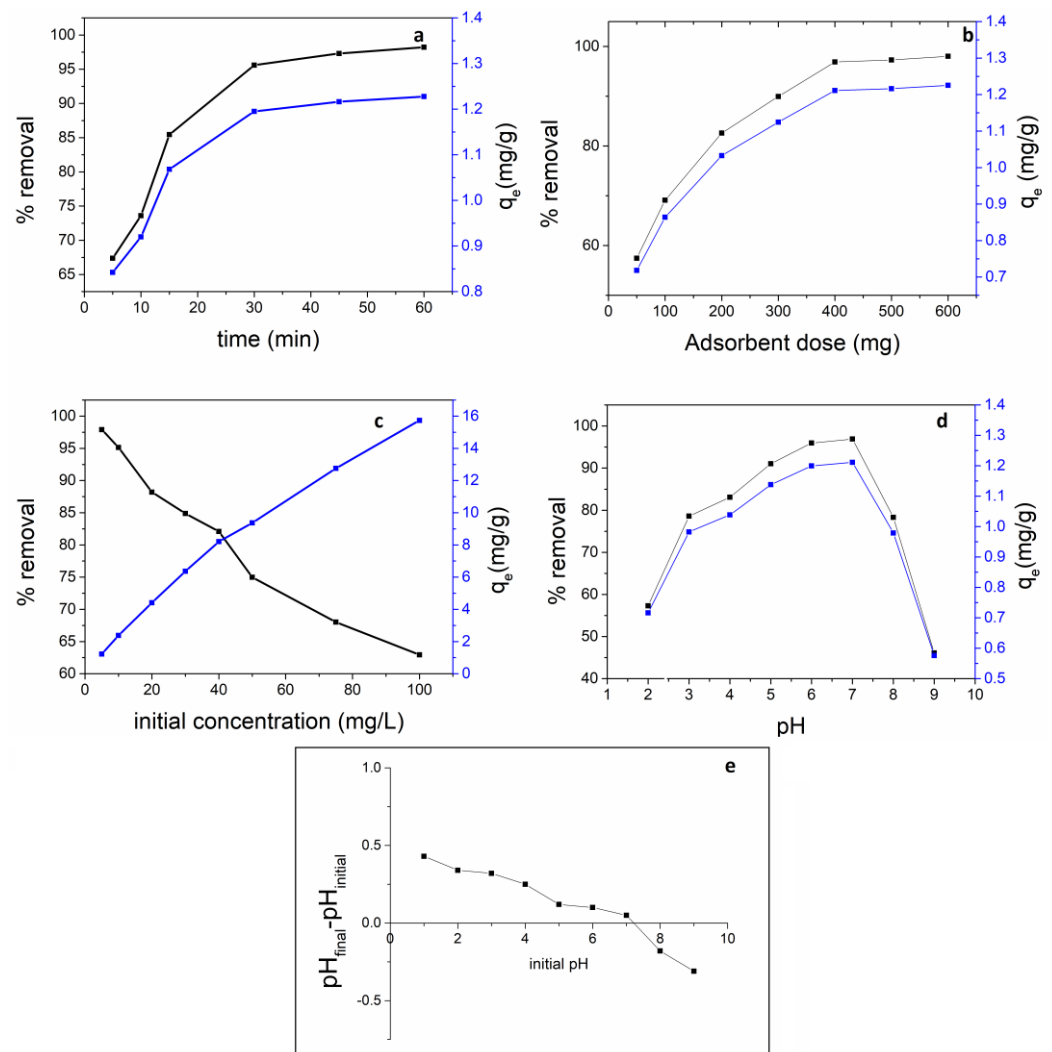
Figure 5. Optimized parameters: (**a**) contact time, (**b**) CSn dose, (**c**) Initial concentration, (**d**) pH, and (**e**) pH point of zero charge.

3.2.2. Effect of Adsorbent Dose

The amount of CSn was varied from 50–600 mg and equilibrated for 45 min with 5 mg/L As(III) at pH 7.0 to study the effect of the adsorbent dose. It was observed that the % removal of As(III) increases with the successive amount of adsorbent (Figure 5b). When the dose of CSn reached 400 mg, there was no observable change in % removal due to the unavailability of As(III) in the solution for incoming rising-adsorption sites on the surface of the CSn [27]. The same results were obtained for the adsorption capacity of CSn towards As(III). Thus, the 400 mg adsorption dose was fixed for further adsorption studies.

3.2.3. Effect of As(III) Concentration

The initial concentration of As(III) was varied in the range of 2–50 mg/L and equilibrated with 400 mg of CSn for 45 min at pH 7.0. At 5 mg/L of As(III), percentage removal was found to be more than 95% and then went on decreasing due to the saturation of adsorption sites on the CSn [28] (Figure 5c). Thus, an initial concentration of 5 mg/L As(III) solution was selected for the adsorption studies. The adsorption capacity of the material went on increasing as the availability of adsorbate increased for the adsorption sites.

3.2.4. Effect of pH

pH and redox potential are the two main factors for arsenic speciation. Speciation of arsenic was sensitive to a pH range of 6.5– 8.5 due to oxidizing and reducing conditions of groundwater. The functionalities present on the surface of adsorbent and adsorbate surfaces are pH-dependent. Therefore, the pH of the media used for the adsorption should be optimized. For this, the pH of 5 mg/L of As(III) solutions was varied from 2.0–9.0 and equilibrated with 400 mg of CSn for 45 min. It was found that maximum percentage removal was observed in the pH range of 6.0–7.0. The pH point of zero charge of CSn was found to be 7.2 (Figure 5e). At a lower pH range, neutral arsenic species (H_3AsO_3) were dominant, whereas the adsorbent CSn surface was highly protonated, which did not favor the As(III) adsorption results in less % removal and low adsorption capacity. The $H_2AsO_3^-$ species of As(III) exists in an alkaline medium. At pH higher than 7.2, the repulsive forces come into action which reduces the % removal of As(III) and CSn has a lower adsorption capacity [29]. Therefore, pH 7.0 is selected for the adsorption of As(III).

3.3. Adsorption Isotherms

Maximum adsorption capacity and monolayer adsorption phenomenon of As(III) on CSn was given by the Langmuir adsorption isotherm [30]. The graph of C_e/q_e vs. C_e (Figure 6a) gives the value for maximum adsorption capacity (q_{max}), and constant b is related to the adsorption energy. Effective interaction between the CSn and As(III) was confirmed by the R_L value, which was found to be lower than the unity. Freundlich [31] adsorption isotherm was studied to understand the heterogeneous adsorption phenomenon of As(III) by CSn. Log q_e vs. Log C_e gives the values for constants k_F and n (Figure 6b). Based on the values of regression, coefficient and comparison graph of experimental q_e along with calculated q_e values for both isotherms against C_e (Figure 6c), point towards the Freundlich isotherm model, which was found to be the best-fitted model for the adsorption process of As(III) on CSn. The equations and results obtained for both isotherms have been depicted in Table 1.

Table 1. Adsorption isotherms and Kinetic model—equations and parameters.

Sr. No.	Models	Parameters	Value
Adsorption Isotherms			
1.	**Langmuir** $\frac{C_e}{q_e} = \frac{1}{q_{max}b} + \frac{C_e}{q_{max}}$ $R_L = \frac{1}{1+bC_0}$	q_{max} (mg g^{-1}) b (L mg^{-1}) R_L r^2	16.64 0.193 0.509 0.955
2.	**Freundlich** $log q_e = \log K_F + \frac{1}{n} log C_e$	K_F (mg$^{1-1/n}$/g/L) n r^2	3.25 2.23 0.994
Kinetic models			
1.	**Pseudo-first-order kinetics** $\log(q_e - q_t) = \log q_e + \frac{k_1 t}{2.303}$	k_1 (min^{-1}) r^2	0.098 0.978
2.	**Pseudo-second-order kinetics** $\frac{t}{q_t} = \frac{1}{k_2 q^2} + \frac{t}{q_e}$	k_2 (g/mg/min) r^2	0.253 0.999
3.	**Intraparticle diffusion** $q_t = k_{int}.t^{\frac{1}{2}} + C$	K_{int} (mg/g/min$^{1/2}$) r^2	0.528 0.523
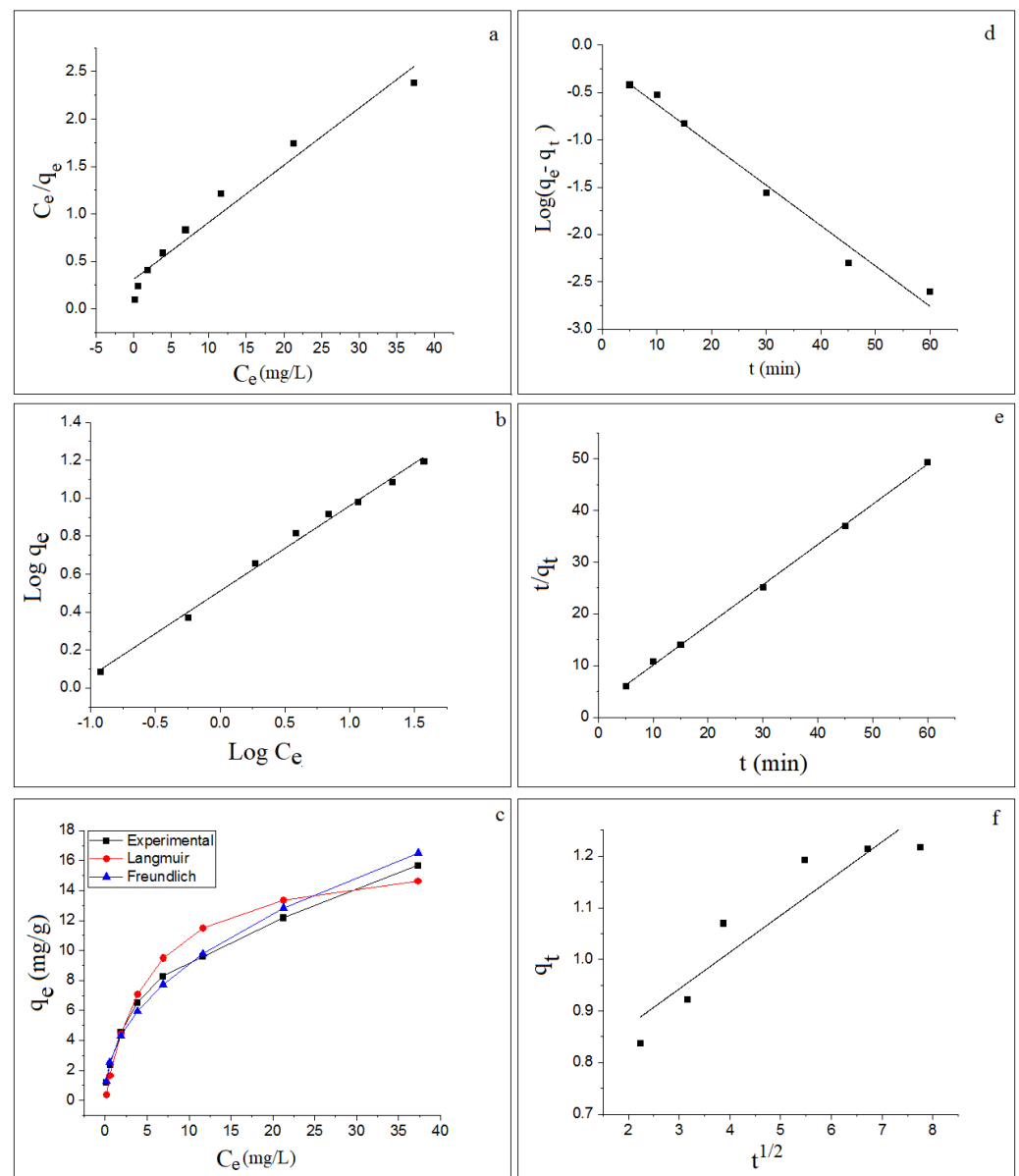
Figure 6. (**a**) Langmuir-adsorption isotherm, (**b**) Freundlich-adsorption isotherm, (**c**) Comparison of isotherms q_e vs. C_e, (**d**) Pseudo-first-order kinetic model, (**e**) Pseudo-second-order kinetic model and (**f**) Weber–Morris model.

3.4. Kinetic Models for Adsorption

Pseudo-first-order kinetic and pseudo-second-order kinetic models (Table 1) were employed to understand the adsorption kinetics of adsorption of As(III) onto the CSn [32]. For this, 50 mL of 5 mg/L As(III) solution was equilibrated with 400 mg of CSn at pH 7.0 for a varied time range of 5–45 min. The pseudo-first-order rate constant (k_1) was obtained through the plot of log ($q_e - q_t$) against t (Figure 6d), while the pseudo-second-order rate constant value was obtained through the plot of t/q_t against t (Figure 6e). Pseudo-second-order kinetic was the best-fit model for the adsorption process of As(III) on CSn, as the value of the correlation coefficient was found to be 0.999 (Table 1).

The adsorption process may proceed through transport in solution bulk, film diffusion, particle diffusion, or with adsorption and desorption within the particles and solid surface. Generally, the diffusion process is considered a rate-limiting step. For this Weber–Morris model was studied to understand whether the diffusion process is a rate-limiting step of

the adsorption process. The non-zero intercept of the linear plot of q_t versus $t^{1/2}$ (Figure 6f) indicates that particle diffusion is not only responsible for the adsorption of As(III) on CSn [33].

3.5. Thermodynamic Study

The effect of temperature on the adsorption process of As(III) on CSn was explained by the thermodynamic parameters studied at temperatures 298 K, 303 K, 308 K, 318 K, and 328 K. The values for ΔH and ΔS (Table 2) were calculated from the slope and intercept of the plot of ln K vs. 1/T (Figure 7), respectively [34]. The spontaneity of the adsorption process was confirmed through the negative value of change in free energyΔG. The value of ΔG was moved towards the positive value with an increase in temperature, indicating that higher temperature does not favor the adsorption process. Negative enthalpy changes ΔH shows the exothermic behavior of the adsorption process. A negative ΔS entropy change value indicates a decrease in the randomness of As(III) as it passes from the solution phase to the CSn surface.

Table 2. Thermodynamic parameters.

Temperature	ΔG (kJ/mol)	ΔH (kJ/mol)	ΔS (kJ/mol/K)
298 K	−15.16		
303 K	−13.96		
308 K	−12.41	−74.946	−0.202
318 K	−10.44		
328 K	−9.228		
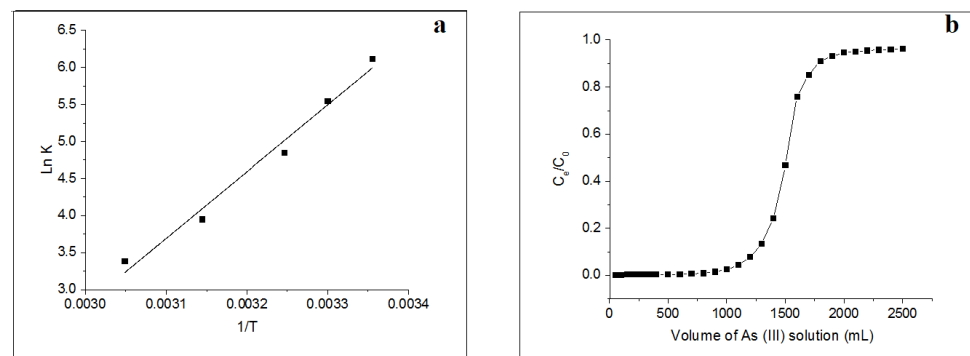
Figure 7. (**a**) Van't Hoff Plot and (**b**) Column study-breakthrough curve.

3.6. Column Studies

For column studies, 1 g of CSn was packed in a glass column of 30.0 cm in length, with an inner diameter of 1.0 cm and a height of 6.0 cm. The flow rate of the column was adjusted to 5 mL/min, and 10 mg/L of As(III) solution was passed through it. The concentration of As(III) in the eluate was analyzed to determine the column efficiency (Figure 7b). Various column parameter values were calculated (Table 3). It was found that compared to batch extraction, the column method is more effective for the treatment of larger sample volumes containing As(III).

Table 3. Column Studies.

Parameter	Result
Inlet concentration of As(III)	10 mg/L
Breakthrough volume	1250 mL
Exhaustion volume	1800 mL
Breakthrough Capacity	12.5 mg/g
Exhaustion Capacity	18 mg/g
Degree of column utilization	69.44

3.7. Effect of Co-Ions

In water samples, various anions were present along with As(III), which may compete for the adsorption sites on CSn during adsorption. To study the effect of co-anions on As(III) removal, solutions of 10 mg/L As(III) with 100 mg/L of each co-anion, such as SO_4^{2-}, Cl^-, PO_4^{3-}, and NO_3^-, were stirred with CSn at optimized conditions for adsorption. Figure 8 shows that the chloride ions have a higher tendency to interfere in the adsorption of As(III) by CSn; as a result, % removal decreases. However, this decrease in the removal tendency of CSn was observed only when chloride ions were present in a ten times higher concentration than As(III).
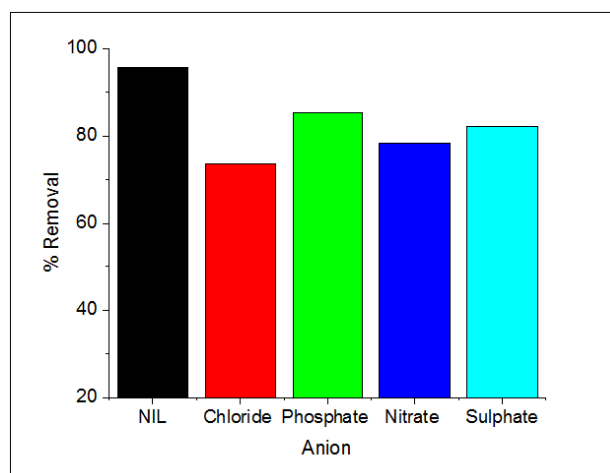

Figure 8. Effect of diverse ions.

3.8. Regeneration and Reusability of Adsorbent

For desorption studies, 5% (*w/v*) of various reagents, such as sodium chloride, sodium nitrate, sodium sulfate, and sodium carbonate, were examined. The best results were obtained with sodium chloride solution (Figure 9). The chloride ions in NaCl exchange with As(III) ions at this higher concentration on the surface of CSn, leading to the desorption of As(III). The regenerated CSn was utilized for ten adsorption–desorption cycles, and it was found that there was a decrease in the percentage removal of As(III) (Figure 9) as compared to the initial CSn. The percentage removal of As(III) was found to be more than 90% for up to three cycles and decreased in successive cycles.
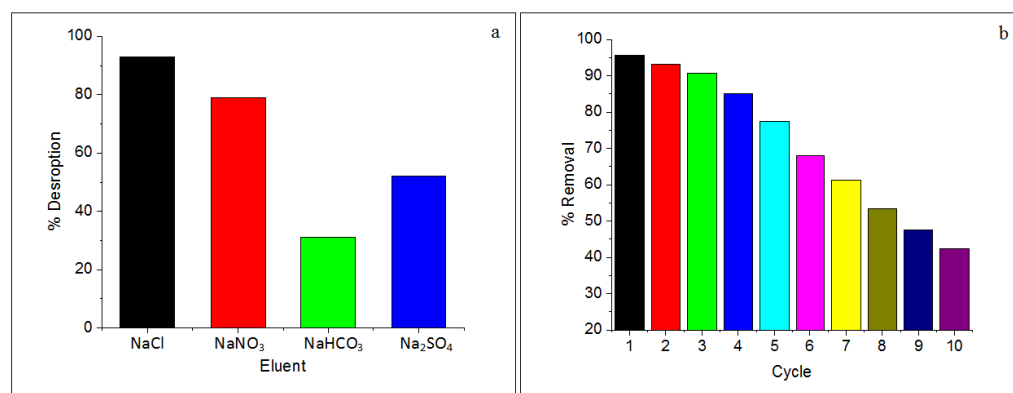

Figure 9. (**a**) Desorption Studies and (**b**) adsorption–desorption cycle.

4. Conclusions

Cellulose biopolymer has a very low adsorption capacity towards As(III). When modified with tin (IV) chloride, it forms a potent biocomposite for As(III). The adsorption

capacity of CSn increased to 16.64 mg/g. The probable mechanism for adsorption includes diffusion and ion exchange of As(III) with chloride ions present on the surface of CSn. Cellulose–tin biocomposite prepared by microwave irradiation, which is different from than conventional method, suggests that the study has a greener aspect. More than 95% adsorption was observed in just 45 min at neutral pH, suggesting that the CSn biocomposite is a very remarkable adsorbent. The isotherm and kinetic data fitted well with the Freundlich isotherm model and pseudo-second-order kinetics, respectively. The thermodynamic studies disclose that the adsorption process is spontaneous and enthalpy-driven. The fixed-bed-column studies suggest that the adsorbent is applicable to a large volume of samples and can be regenerated and reused multiple times.

Author Contributions: A.S.—Conceptualization and writing original draft, R.J.—supervision and visualization. V.G. and S.P.—writing, review, and editing, S.K.—methodology, and S.D.—resources. All authors have read and agreed to the published version of the manuscript.

Conflicts of Interest: The authors declare no conflict of interest.

References

1. Baghaei, B.; Skrifvars, M. All-Cellulose Composites: A Review of Recent Studies on Structure, Properties and Applications. *Molecules* **2020**, *25*, 2836. [CrossRef] [PubMed]
2. Xie, Y.; Gao, S.; Ling, Z.; Lai, C.; Huang, Y.; Wang, J.; Wang, C.; Chu, F.; Xu, F.; Dumont, M.-J.; et al. A Multiscale Biomimetic Strategy to Design Strong, Tough Hydrogels by Tuning the Self-Assembly Behavior of Cellulose. *J. Mater. Chem. A* **2022**, *10*, 13685–13696. [CrossRef]
3. Fernandes, S.C.; Freire, C.S.; Silvestre, A.J.; Pascoal Neto, C.; Gandini, A. Novel Materials Based on Chitosan and Cellulose: Novel Materials Based on Chitosan and Cellulose. *Polym. Int.* **2011**, *60*, 875–882. [CrossRef]
4. Egor, M.; Kumar, A.A.; Ahuja, T.; Mukherjee, S.; Chakraborty, A.; Sudhakar, C.; Srikrishnarka, P.; Bose, S.; Ravindran, S.J.; Pradeep, T. Cellulosic Ternary Nanocomposite for Affordable and Sustainable Fluoride Removal. *ACS Sustain. Chem. Eng.* **2021**, *9*, 12788–12799. [CrossRef]
5. Pinto, R.J.B.; Neves, M.C.; Neto, C.P.; Trindade, T.; Pinto, R.J.B.; Neves, M.C.; Neto, C.P.; Trindade, T. *Composites of Cellulose and Metal Nanoparticles*; IntechOpen: London, UK, 2012; ISBN 978-953-51-0762-0.
6. Pandey, S. A comprehensive review on recent developments in bentonite based materials used as adsorbents for wastewater treatment. *J. Mol. Liq.* **2017**, *241*, 1091–1113. [CrossRef]
7. Shekhawat, A.; Kahu, S.S.; Saravanan, D.; Jugade, R.M. Assimilation of Chitin with Tin for Defluoridation of Water. *RSC Adv.* **2016**, *6*, 18936–18945. [CrossRef]
8. Shekhawat, A.; Kahu, S.; Saravanan, D.; Jugade, R. Tin(IV) Cross-Linked Chitosan for the Removal of As(III). *Carbohydr. Polym.* **2017**, *172*, 205–212. [CrossRef]
9. Yamani, J.S.; Miller, S.M.; Spaulding, M.L.; Zimmerman, J.B. Enhanced Arsenic Removal Using Mixed Metal Oxide Impregnated Chitosan Beads. *Water Res.* **2012**, *46*, 4427–4434. [CrossRef]
10. Borah, G.; Mudoi, P.P.; Borah, P. Chapter 13—Arsenic Contamination in Water Resources and Its Health Risk Assessment. In *Contamination of Water*; Ahamad, A., Siddiqui, S.I., Singh, P., Eds.; Academic Press: Cambridge, MA, USA, 2021; pp. 187–198. ISBN 978-0-12-824058-8.
11. Ghosh, N.C. *Groundwater Arsenic Contamination in India: Vulnerability and Scope for Remedy*; National Institute of Hydrology: Roorke, India, 2010.
12. Liu, B.; Kim, K.-H.; Kumar, V.; Kim, S. A Review of Functional Sorbents for Adsorptive Removal of Arsenic Ions in Aqueous Systems. *J. Hazard. Mater.* **2020**, *388*, 121815. [CrossRef]
13. Weerasundara, L.; Ok, Y.-S.; Bundschuh, J. Selective Removal of Arsenic in Water: A Critical Review. *Environ. Pollut.* **2021**, *268*, 115668. [CrossRef]
14. Khapre, M.A.; Jugade, R.M. Hierarchical Approach towards Adsorptive Removal of Alizarin Red S Dye Using Native Chitosan and Its Successively Modified Versions. *Water Sci. Technol.* **2020**, *82*, 715–731. [CrossRef] [PubMed]
15. Khapre, M.; Shekhawat, A.; Saravanan, D.; Pandey, S.; Jugade, R. Mesoporous Fe–Al-Doped Cellulose for the Efficient Removal of Reactive Dyes. *Mater. Adv.* **2022**, *3*, 3278–3285. [CrossRef]
16. Araga, R.; Sharma, C.S. Amine Functionalized Electrospun Cellulose Nanofibers for Fluoride Adsorption from Drinking Water. *J Polym. Environ.* **2019**, *27*, 816–826. [CrossRef]

17. Eltaweil, A.S.; Abd El-Monaem, E.M.; El-Subruiti, G.M.; Ali, B.M.; Abd El-Latif, M.M.; Omer, A.M. Graphene Oxide Incorporated Cellulose Acetate Beads for Efficient Removal of Methylene Blue Dye; Isotherms, Kinetic, Mechanism and Co-Existing Ions Studies. *J Porous. Mater.* **2022**. [CrossRef]
18. Kahu, S.; Shekhawat, A.; Saravanan, D.; Jugade, R. Stannic Chloride Impregnated Chitosan for Defluoridation of Water. *Int. J. Biol. Macromol.* **2017**, *104*, 1528–1538. [CrossRef]
19. Bullen, J.C.; Lapinee, C.; Miller, L.A.; Bullough, F.; Berry, A.J.; Najorka, J.; Cibin, G.; Vilar, R.; Weiss, D.J. Spectroscopic (XAS, FTIR) Investigations into Arsenic Adsorption onto TiO2/Fe2O3 Composites: Evaluation of the Surface Complexes, Speciation and Precipitation Predicted by Modelling. *Results Surf. Interfaces* **2022**, *9*, 100084. [CrossRef]
20. Srivastava, N.; Mukhopadhyay, M. Biosynthesis of SnO $_2$ Nanoparticles Using Bacterium *Erwinia Herbicola* and Their Photocatalytic Activity for Degradation of Dyes. *Ind. Eng. Chem. Res.* **2014**, *53*, 13971–13979. [CrossRef]
21. Segal, L.; Creely, J.J.; Martin, A.E.; Conrad, C.M. An Empirical Method for Estimating the Degree of Crystallinity of Native Cellulose Using the X-Ray Diffractometer. *Text. Res. J.* **1959**, *29*, 786–794. [CrossRef]
22. Leal, G.F.; Ramos, L.A.; Barrett, D.H.; Curvelo, A.A.S.; Rodella, C.B. A Thermogravimetric Analysis (TGA) Method to Determine the Catalytic Conversion of Cellulose from Carbon-Supported Hydrogenolysis Process. *Thermochim. Acta* **2015**, *616*, 9–13. [CrossRef]
23. Jabareen, L.; Maruthapandi, M.; Saravanan, A.; Gedanken, A. Effective Degradation of Cellulose by Microwave Irradiation in Alkaline Solution. *Cellulose* **2021**, *28*, 11275–11285. [CrossRef]
24. Yadav, M. Study on Thermal and Mechanical Properties of Cellulose/Iron Oxide Bionanocomposites Film. *Compos. Commun.* **2018**, *10*, 1–5. [CrossRef]
25. Sankararamakrishnan, N.; Srivastava, I.; Mishra, S. Studies on Novel Nano-Bimetal Doped Cellulose Nanofibers Derived from Agrowaste towards Deflouridation. *Int. J. Biol. Macromol.* **2019**, *128*, 556–565. [CrossRef] [PubMed]
26. Kahu, S.; Shekhawat, A.; Saravanan, D.; Jugade, R. Ionic Solid-Impregnated Sulphate-Crosslinked Chitosan for Effective Adsorption of Hexavalent Chromium from Effluents. *Int. J. Environ. Sci. Technol.* **2016**, *13*, 2269–2282. [CrossRef]
27. Gomase, V.; Jugade, R.; Doondani, P.; Deshmukh, S.; Saravanan, D.; Pandey, S. Dual Modifications of Chitosan with PLK for Amputation of Cyanide Ions: Equilibrium Studies and Optimization Using RSM. *Int. J. Biol. Macromol.* **2022**, *223*, 636–651. [CrossRef]
28. Shekhawat, A.; Kahu, S.; Saravanan, D.; Pandey, S.; Jugade, R. Rational Modification of Chitosan Biopolymer for Remediation of Cr(VI) from Water. *J. Hazard. Mater. Adv.* **2022**, *7*, 100123. [CrossRef]
29. Singh, D.B.; Prasad, G.; Rupainwar, D.C.; Singh, V.N. As(III) Removal from Aqueous Solution by Adsorption. *Water Air Soil Pollut.* **1988**, *42*, 373–386. [CrossRef]
30. Langmuir, I. The adsorption of gases on plane surfaces of glass, mica and platinum. *J. Am. Chem. Soc.* **1918**, *40*, 1361–1403. [CrossRef]
31. Freundlich, H. Über Die Adsorption in Lösungen. *Z. Für Phys. Chem.* **1907**, *57U*, 385–470. [CrossRef]
32. Azizian, S.; Eris, S. Adsorption Isotherms and Kinetics. In *Interface Science and Technology, Volume 3*; Elsevier: Amsterdam, The Netherlands, 2021; pp. 445–509; ISBN 978-0-12-818805-7.
33. Campos, N.F.; Barbosa, C.M.; Rodríguez-Díaz, J.M.; Duarte, M.M. Removal of Naphthenic Acids Using Activated Charcoal: Kinetic and Equilibrium Studies. *Adsorpt. Sci. Technol.* **2018**, *36*, 1405–1421. [CrossRef]
34. Korde, S.; Tandekar, S.; Jugade, R.M. Novel Mesoporous Chitosan-Zirconia-Ferrosoferric Oxide as Magnetic Composite for Defluoridation of Water. *J. Environ. Chem. Eng.* **2020**, *8*, 104360. [CrossRef]